

Active control of near-field coupling in conductively coupled microelectromechanical system metamaterial devices

Prakash Pitchappa, Manukumara Manjappa, Chong Pei Ho, You Qian, Ranjan Singh, Navab Singh, and Chengkuo Lee

Citation: [Applied Physics Letters](#) **108**, 111102 (2016); doi: 10.1063/1.4943974

View online: <http://dx.doi.org/10.1063/1.4943974>

View Table of Contents: <http://scitation.aip.org/content/aip/journal/apl/108/11?ver=pdfcov>

Published by the [AIP Publishing](#)

Articles you may be interested in

[Resonance tuning due to Coulomb interaction in strong near-field coupled metamaterials](#)

J. Appl. Phys. **118**, 023104 (2015); 10.1063/1.4926758

[Lessons learned for implementing near-field active control systems to achieve global control of fan noise](#)

J. Acoust. Soc. Am. **131**, 3379 (2012); 10.1121/1.4708741

[Analysis of near-field control in a single-nanoparticle system](#)

AIP Conf. Proc. **1176**, 149 (2009); 10.1063/1.3253893

[Active control of free-field sound using near-field energy-based error signals](#)

J. Acoust. Soc. Am. **120**, 3198 (2006); 10.1121/1.4788069

[Field emission characteristics of a tungsten microelectromechanical system device](#)

Appl. Phys. Lett. **86**, 153502 (2005); 10.1063/1.1875756

The advertisement features a white Lake Shore Model 372 cryogenic temperature controller on the left. The device has a digital display showing '98.837' and a keypad with various function buttons. To the right is a detailed, close-up view of a cryogenic system, showing a complex arrangement of metal pipes, valves, and a large cylindrical component, likely a cryostat. The background is a gradient of blue. The text 'Precise temperature control for cryogenic research' is written in white on the left, and the 'Lake Shore CRYOTRONICS' logo is in the top right corner.

Precise temperature control
for cryogenic research

Model 372

Lake Shore
CRYOTRONICS

Active control of near-field coupling in conductively coupled microelectromechanical system metamaterial devices

Prakash Pitchappa,^{1,2} Manukumara Manjappa,³ Chong Pei Ho,^{1,2} You Qian,^{1,2} Ranjan Singh,³ Navab Singh,⁴ and Chengkuo Lee^{1,2,a)}

¹NUS Suzhou Research Institute (NUSRI), Suzhou, Industrial Park, Suzhou 215123, People's Republic of China

²Center for Intelligent Sensors and MEMS, Department of Electrical and Computer Engineering, National University of Singapore, 4 Engineering Drive 3, Singapore 117576

³Division of Physics and Applied Physics, Centre for Disruptive Photonic Technologies, School of Physical and Mathematical Sciences, Nanyang Technological University, Singapore 637371

⁴Institute of Microelectronics (IME), 11 Science Park Road, Singapore 117685

(Received 31 January 2016; accepted 2 March 2016; published online 15 March 2016)

We experimentally report a structurally reconfigurable metamaterial for active switching of near-field coupling in conductively coupled, orthogonally twisted split ring resonators (SRRs) operating in the terahertz spectral region. Out-of-plane reconfigurable microcantilevers integrated into the dark SRR geometry are used to provide active frequency tuning of dark SRR resonance. The geometrical parameters of individual SRRs are designed to have identical inductive-capacitive resonant frequency. This allows for the excitation of classical analogue of electromagnetically induced transparency (EIT) due to the strong conductive coupling between the SRRs. When the microcantilevers are curved up, the resonant frequency of dark SRR blue-shifts and the EIT peak is completely modulated while the SRRs are still conductively connected. EIT modulation contrast of $\sim 50\%$ is experimentally achieved with actively switchable group delay of ~ 2.5 ps. Electrical control, miniaturized size, and readily integrable fabrication process of the proposed structurally reconfigurable metamaterial make it an ideal candidate for the realization of various terahertz communication devices such as electrically controllable terahertz delay lines, buffers, and tunable data-rate channels. © 2016 AIP Publishing LLC. [<http://dx.doi.org/10.1063/1.4943974>]

The ever-increasing demand for faster data rates is currently pushing the wireless communication to sub-terahertz frequencies.^{1,2} Slow light devices is a critical part in the development of various terahertz (THz) communication devices such as modulators, optical buffers, delay-lines, and tunable bandwidth filters. However, THz waves lie in between the electronics and photonic realms of the electromagnetic spectrum and also greatly lack naturally occurring materials that would strongly interact with these waves.³ Artificially engineered materials known as metamaterials have aided in bridging the so called “THz gap” over the past decade.^{4–6} Interestingly, planar metamaterials have been reported to achieve classical analogue of electromagnetically induced transparency (EIT) phenomenon, which provides an access route for slow light behavior in a desired spectral region.^{7–12} EIT analogue in metamaterial is typically realized through the excitation of sharp radiative mode resonance in the dark resonator amid a broader absorption spectra of the bright resonator by virtue of near-field coupling.

Active control of EIT analogue in metamaterial would enable tunable group-delay that is highly desirable for practical applications. One of three primary parameters in the near-field coupled metamaterials—bright mode resonance frequency, dark mode resonance frequency, or intercoupling distance between the resonators—can be altered to achieve active control of EIT bandwidth, intensity, and frequency. Earlier reports on active control of EIT analogue in metamaterial predominantly utilize optically controlled

photoconductive materials that are integrated either into resonator geometry^{13,14} or intercoupling space¹⁵ or directly used as substrate or surrounding medium.^{16–19} Thermally controlled superconductors are also reported for active modulation of EIT analogue in planar metamaterials.^{20–22} However, the scalability of these tunable approaches are limited, owing to the frequency dependent material properties of the active materials. Also, some of these approaches demand for exotic materials that are difficult to process or require bulky experimental setup to provide control signals. Alternatively, microelectromechanical system (MEMS) based structurally reconfigurable metamaterials are proposed as the most straightforward and efficient means of achieving active control in THz metamaterials.^{23–31} The MEMS metamaterials are also reported for active control of EIT analogue in inductively coupled systems.^{32,33} The in-plane reconfigurable metamaterial is numerically studied to achieve active modulation of EIT analogue by continuously varying the intercoupling distance between the resonators,³² while the out-of-plane reconfigurable metamaterial with independent control of constituent resonators was reported to achieve both EIT modulation and spectral tuning.³³ However, these reports are demonstrated for inductively coupled systems, where the resonators are coupled via near-field coupling across a small spatial gap. The strongest coupling occurs in conductively coupled resonator system,³⁴ and active switching of conductive coupling between the resonators would enable high-performance slow light characteristics, which is critical for practical THz applications.

^{a)}elelc@nus.edu.sg

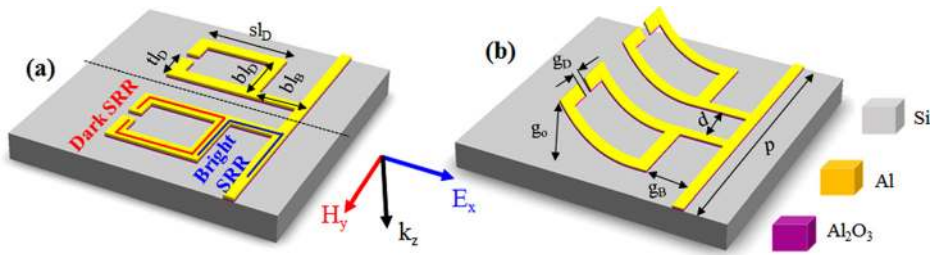


FIG. 1. Schematics of the conductively coupled MEMS metamaterial in (a) ON state and (b) OFF state with geometrical parameter definitions.

In this report, active switching of near-field coupling in conductively coupled split ring resonators (SRRs) placed in orthogonally twisted fashion is experimentally demonstrated in the THz spectral region. The bright and dark SRRs are designed to have identical resonant frequency and hence enable the excitation of EIT analogue at 0.68 THz by virtue of conductive coupling of dark SRR to the bright SRR. Out-of-plane reconfigurable microcantilevers are integrated into the dark SRR geometry, which enables the active sweep of the dark mode resonant frequency. Due to the mismatch between the bright and dark resonant frequencies, the system switches from strongly coupled to uncoupled state, even when they are physically connected to each other at all times. The active switching of near-field coupling provides electrically tunable group delay, which are critical for development of THz communication devices.

The MEMS metamaterial unit cell consists of two conductively coupled SRRs that are orthogonally twisted with respect to each other as shown in Fig. 1(a). The bright SRR is completely fixed to the substrate, while the side arms along with the tip forming split gap of the dark resonator are released from the substrate plane to provide active reconfiguration. One of the side arms of bright SRR also acts as the base of dark SRR and forms the conductive path for electrical control signal to actively reconfigure the dark SRR cantilevers. The geometrical parameters of the SRRs are shown in Fig. 1(b).

The polarization of the incident THz wave is along the gap-bearing side of the bright SRR, i.e., along x -direction and hence enables the direct excitation of fundamental inductive-capacitive (LC) mode resonance of the bright SRR.³⁵ However, for this polarization of THz incidence, LC mode resonance of dark SRR is not directly accessible.³⁵ In order to achieve strong coupling between the resonators, the resonant frequency of the bright and dark SRRs should be identical. In the earlier reports using inductively coupled orthogonal twisted SRRs, the same geometrical dimensions are used for both SRRs.^{14,36} However, in our case, the resonant

frequency of SRRs will be influenced by the routing lines and shared geometry with the other SRR. Detailed finite difference time domain (FDTD) simulations were performed using Computer Software Technology (CST) Microwave studio 2009 to ensure that the resonances of individual bright and dark mode resonator are identical and to elucidate the effect of sweeping the dark mode resonance away from the bright mode in the coupled system. The SRRs are made of bilayer materials – 500 nm aluminum (Al) on top of 50 nm aluminum oxide (Al_2O_3) on top of silicon (Si) substrate. Al was modelled as lossy metal with conductivity of 1×10^7 S/m. Al_2O_3 and Si were modelled as lossless dielectric with dielectric constants of 9.5 and 11.9, respectively. In the simulation, a single unit cell of the metamaterial structure was simulated with periodic boundary conditions employed in axial directions orthogonal to the incident waves. The perfectly matched layers are applied along the propagation of the electromagnetic waves. Plane waves were incident onto the unit cell from the port on the metal side, while the transmission spectrum was determined from the port placed at the other side of metamaterial.

The bright SRR is built with the following geometrical dimension of base length (bl_B) = $5 \mu\text{m}$, side arm length (sl_B) = $20 \mu\text{m}$, and split gap (g_B) = $5 \mu\text{m}$. The simulated transmission spectra for individual bright SRR with metal line are shown in Fig. 2(a) for incident THz waves with electric field polarized along the gap of the SRR. It can be seen that there is a strong resonance dip at 0.68 THz and the circulating surface current configuration shown in the inset confirms the excitation of the LC mode resonance. The geometrical parameters of the dark mode SRR were optimized to have the base length (bl_D) = $20 \mu\text{m}$, side arm length (sl_D) = $25 \mu\text{m}$, tip length (tl_D) = $3 \mu\text{m}$, and the split gap (g_D) = $3 \mu\text{m}$ in order to achieve the same resonance frequency as the bright SRR. The THz wave was incident with E field along the y -direction, which is along the gap bearing size of the dark SRR and the simulated transmission spectrum of dark with varying release angle of the microcantilevers is shown in Fig. 2(b). It can be seen that

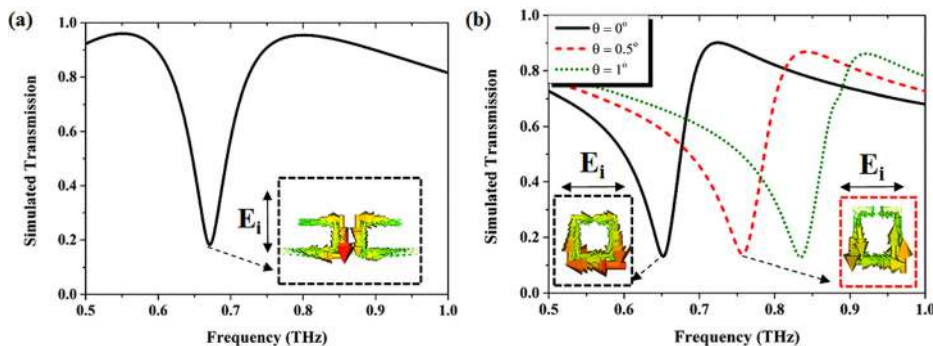


FIG. 2. Simulated transmission response of (a) bright SRR for the incident electric field along the gap bearing side and the inset shows the induced circulating current at the resonance frequency, indicating the excitation of LC mode resonance and (b) dark SRR for the incident electric field along the gap bearing side at varying release angle (θ) and the insets show the induced surface current at respective resonant frequency.

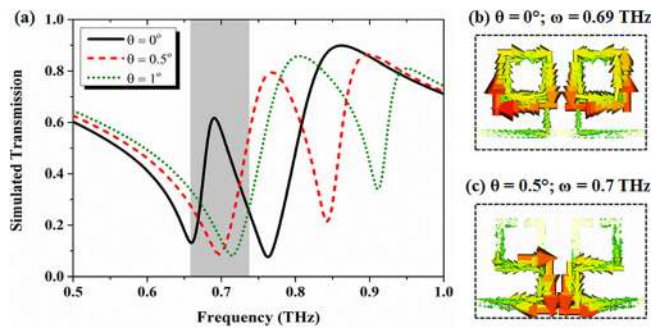


FIG. 3. (a) Simulated transmission response of conductively coupled MEMS metamaterial with varying release angle (θ) of dark SRR cantilevers. Simulated surface current at 0.68 THz for the conductively coupled MEMS metamaterial in (b) ON state and (c) OFF state, respectively.

when the release angle, $\theta = 0^\circ$, the resonant frequency is at 0.68 THz and matches well with the LC mode resonance of bright SRR. As the angle increases, the gap between the microcantilever and Si substrate increases and causes the effective capacitance of SRR to decrease, thereby causing the blue shift of the resonant frequency of dark SRR as shown in Fig. 2(b).^{27,37}

The transmission response of conductively coupled SRRs was simulated for different release angles of dark SRR cantilevers at normal incidence with THz electric field polarized along the gap of bright SRR (E_x) as shown in Fig. 3(a). It can be observed that when the $\theta = 0^\circ$, there is a sharp transmission peak amid the absorption spectrum at 0.68 THz. The strong circulating current in the dark SRR simulated at 0.68 THz shown in Fig. 3(b) indicates the excitation of dark SRR due to the strong conductive coupling of dark SRR with the bright SRR.³⁴ As the angle increases, the resonant frequency of the dark SRR blue shifts and the mismatch between the bright and dark resonances significantly weakens the coupling between the resonators, thereby causing the EIT peak to be strongly modulated at 0.68 THz. Even for $\theta = 0.5^\circ$ release angle, the circulating surface current configuration in the bright SRR at the transmission dip at 0.68 THz as shown in Fig. 3(c) confirms the direct excitation of LC mode resonance of bright SRR and the reduced influence of dark SRR. Hence, the proposed MEMS metamaterial provides an efficient means of actively modulating the near-field coupling between the conductively coupled resonators.

The SRRs are made of bilayer materials—500 nm aluminum (Al) on top of 50 nm aluminum oxide (Al_2O_3) fabricated on lightly doped silicon (Si) substrate using complementary

metal-oxide-semiconductor compatible process.³⁸ Silicon-dioxide (SiO_2) is used as the sacrificial layer. The side arms of dark SRRs are released by isotropic etching of SiO_2 layer underneath these structures. The residual stress in the bi-material layers will cause the released cantilevers to curve up in the out-of-plane direction, thereby increasing the initial air gap between the released cantilever and Si substrate (g_0) to be $2.2 \mu\text{m}$, which is much higher than the sacrificial layer thickness of 100 nm. The upward curvature of the released cantilever can be clearly seen in the optical image of the fabricated MEMS metamaterial shown in Fig. 4. In order to actively reconfigure the physical position of the microcantilevers, electrostatic actuation by applying voltage across the released microcantilevers and Si substrate is used. The attractive electrostatic force causes the microcantilevers to deform towards the fixed substrate. This physical deformation generates the restoring force, which opposes the deformation of microcantilevers towards the substrate. Hence, the position of microcantilever is defined by the balance between the attractive electrostatic force and restoring force. As the voltage is increased, the electrostatic force increases sharply compared to the restoring force. Hence, after a particular value of input voltage called the “Pull-in voltage,” the electrostatic force will be much higher than the restoring force, thereby forcing the microcantilever to come in physical contact with Si substrate.^{39,40} Based on the input voltage, two states are defined as OFF state when no voltage is applied and ON state when the input voltage is higher than the pull-in voltage. The rest state of the cantilevers after fabrication will be the OFF state, where there will be an airgap between the released cantilevers and Si substrate. When the microcantilevers are reconfigured to ON states, the cantilevers are in physical contact with the Si substrate. The deformation profile of the microcantilevers is characterized using Lyncee Tec. Reflection Digital Holographic Microscope. The 3D profile of the device in OFF state confirms the out-of-plane deformation of released cantilevers as shown in Fig. 5. The measured phase of the curved up cantilever in OFF state and flat cantilever in ON state is shown as insets in Fig. 5. The negative displacement in the ON state corresponds to the thickness of sacrificial layer of 100 nm, which is removed during the release step.

THz time domain spectroscopy (THz-TDS) is used to characterize the THz transmission response of the fabricated metamaterial in different reconfiguration states. THz wave at normal incidence interacts with the sample with predetermined

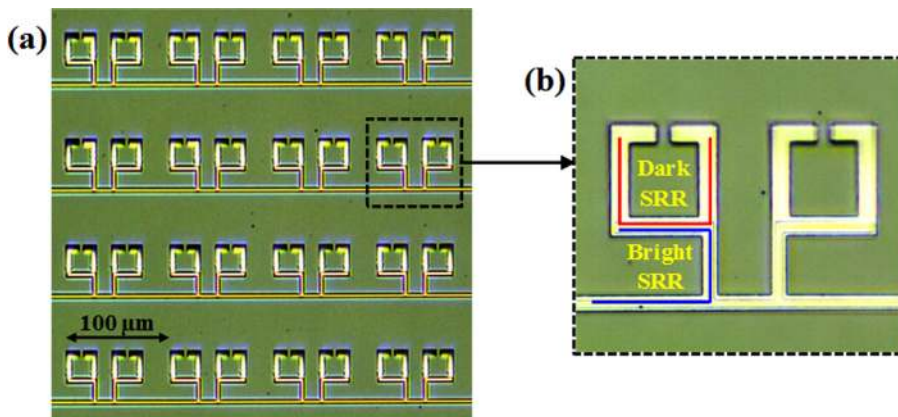


FIG. 4. (a) Optical microscope (OM) image of the conductively coupled MEMS metamaterial with curved up cantilevers and (b) zoomed in OM image of conductively coupled MEMS metamaterial unit cell.

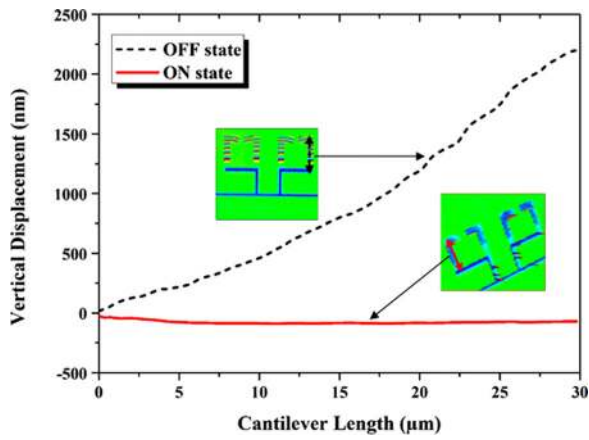


FIG. 5. Measured cantilever deformation in OFF state (black-dashed curve) and ON state (red-solid curve) with the phase figures of each state shown in insets.

polarization (x-polarization). The released metamaterial chip is bonded to a printed circuit board with a hole of 1 cm x 1 cm in center. The bonded sample is then placed in the nitrogen-filled chamber of the THz-TDS setup. The dark SRR microcantilever is biased with positive potential, while Si substrate is kept as ground terminal. The measured transmission through fabricated MEMS metamaterial is then normalized with transmission through bare Si substrate of same thickness as the samples. The measured transmission spectrum at ON and OFF states of dark SRR is shown in Fig. 6(a). It can be observed that in the ON state, the EIT peak occurs at 0.69 THz which is completely modulated in comparison to the microcantilevers in the OFF state. The measured transmission spectra in ON and OFF states match quite well with the simulated data. EIT modulation of $\sim 50\%$ is experimentally achieved at 0.68 THz. The active modulation of the transmission properties of the coupled system is used to demonstrate the active control of the slow light behavior in the conductively coupled systems. The group delay for the pulses is given by $t_g = -d\phi/d\omega$, where ϕ is the phase and ω is the angular frequency of the pulse. Fig. 6(b) shows experimentally measured group delay of the THz pulses propagating through the MEMS metamaterial in ON and OFF states, which depict the group delay of the THz pulse in the system. It can be seen that in the ON state, due to excitation of EIT, the group delay of ~ 2.5 ps is achieved, which disappears when the cantilevers are switched to OFF state. The delay band width product (DBP) defined as the product of maximum group delay and the spectrum bandwidth ($DBP = t_g \times \Delta f$) is calculated for the proposed samples. DBP is a figure of merit to determine the efficiency of the devices for telecommunication channels, where the maximum DBP implies that the device is more efficient to store and transmit the information through the signal channel. The measured DBP for the sample in the ON state is calculated to be 0.117 and for the OFF state the system shows complete absorption leading to the losses in the transmission channel. Thus, the information carrying bandwidth of a transmission network could be actively controlled that would enable an accurate control/modulation of the amount of information/bit volume through the telecom channel. Thus, the proposed MEMS metamaterial can be used as an active switch of DBP through the transmission line. This

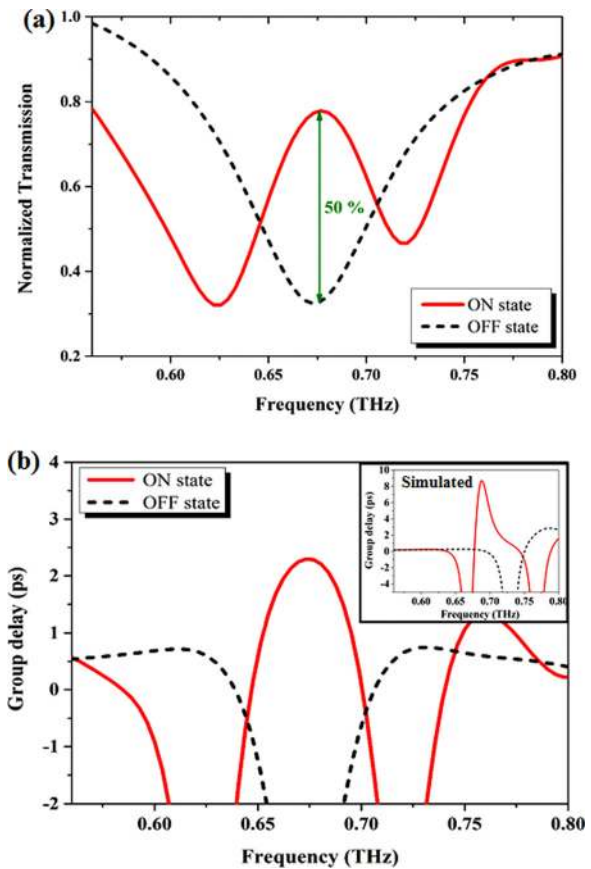


FIG. 6. (a) Measured THz transmission response and (b) Measured (inset-simulated) group delay of conductively coupled MEMS metamaterial in OFF state (black-dashed curve) and ON state (red-solid curve), respectively.

strong electro-optic performance achieved through active reconfiguration of conductively coupled resonators aids in the realization of efficient THz slow light devices. Furthermore, conductively coupled SRRs are proposed as a path to achieve high Q systems,⁴¹ and the proposed MEMS approach can be readily integrated into these metamaterials to provide tunable high Q factor devices, as well.

In summary, a structurally reconfigurable metamaterial is experimentally demonstrated for active switching of near-field coupling in conductively coupled resonators system. Complete modulation of EIT analogue was achieved through active spectral sweeping of the dark mode resonance relative to the bright mode resonance. Electrically tunable group delay of 2.5 ps and active switching of delay bandwidth product is experimentally achieved. The proposed metamaterial is electrically controlled, highly miniaturized, and can be easily integrated with integrated circuits to provide active control signals. This makes the proposed MEMS metamaterial to be the ideal candidate for the realization of wide range of miniaturized slow light THz devices such as modulators, buffers, and optical delays.

The authors acknowledge the financial support from the research grant of, MOE/NUS; ARF-Tier 2 (MOE2012-T2-2-154) "Monolithic integrated Si/AlN nanophotonics platform for optical NEMS and OEICs" at the National University of Singapore; and partially supported by National Natural Science Foundation of China under Grant No. 61474078 at NUS (Suzhou) Research Institute, Suzhou, China.

- ¹S. Koenig, D. Lopez-Diaz, J. Antes, F. Boes, R. Henneberger, A. Leuther, A. Tessmann, R. Schmogrow, D. Hillerkuss, and R. Palmer, *Nat. Photonics* **7**, 977 (2013).
- ²J. Federici and L. Moeller, *J. Appl. Phys.* **107**, 111101 (2010).
- ³B. Ferguson and X.-C. Zhang, *Nat. Mater.* **1**, 26 (2002).
- ⁴T.-J. Yen, W. Padilla, N. Fang, D. Vier, D. Smith, J. Pendry, D. Basov, and X. Zhang, *Science* **303**, 1494 (2004).
- ⁵H. Tao, N. I. Landy, C. M. Bingham, X. Zhang, R. D. Averitt, and W. J. Padilla, *Opt. Express* **16**, 7181 (2008).
- ⁶W. Withayachumnankul and D. Abbott, *IEEE Photonics J.* **1**, 99 (2009).
- ⁷N. Papasimakis, V. A. Fedotov, N. Zheludev, and S. Prosvirnin, *Phys. Rev. Lett.* **101**, 253903 (2008).
- ⁸S. Zhang, D. A. Genov, Y. Wang, M. Liu, and X. Zhang, *Phys. Rev. Lett.* **101**, 047401 (2008).
- ⁹P. Tassin, L. Zhang, T. Koschny, E. Economou, and C. M. Soukoulis, *Phys. Rev. Lett.* **102**, 053901 (2009).
- ¹⁰S.-Y. Chiam, R. Singh, C. Rockstuhl, F. Lederer, W. Zhang, and A. A. Bettiol, *Phys. Rev. B* **80**, 153103 (2009).
- ¹¹P. Tassin, L. Zhang, T. Koschny, E. Economou, and C. M. Soukoulis, *Opt. Express* **17**, 5595 (2009).
- ¹²N. Liu, L. Langguth, T. Weiss, J. Kästel, M. Fleischhauer, T. Pfau, and H. Giessen, *Nat. Mater.* **8**, 758 (2009).
- ¹³J. Gu, R. Singh, X. Liu, X. Zhang, Y. Ma, S. Zhang, S. A. Maier, Z. Tian, A. K. Azad, and H.-T. Chen, *Nat. Commun.* **3**, 1151 (2012).
- ¹⁴D. R. Chowdhury, R. Singh, A. J. Taylor, H.-T. Chen, and A. K. Azad, *Appl. Phys. Lett.* **102**, 011122 (2013).
- ¹⁵X. Su, C. Ouyang, N. Xu, S. Tan, J. Gu, Z. Tian, R. Singh, S. Zhang, F. Yan, and J. Han, *Sci. Rep.* **5**, 10823 (2015).
- ¹⁶Y. Zhu, X. Hu, Y. Fu, H. Yang, and Q. Gong, *Sci. Rep.* **3**, 2338 (2013).
- ¹⁷F. Miyamaru, H. Morita, Y. Nishiyama, T. Nishida, T. Nakanishi, M. Kitano, and M. W. Takeda, *Sci. Rep.* **4**, 4346 (2014).
- ¹⁸X. Yang, J. Yang, X. Hu, Y. Zhu, H. Yang, and Q. Gong, *Appl. Phys. Lett.* **107**, 081110 (2015).
- ¹⁹Y. Bai, K. Chen, H. Liu, T. Bu, B. Cai, J. Xu, and Y. Zhu, *Opt. Commun.* **353**, 83 (2015).
- ²⁰J. Wu, B. Jin, J. Wan, L. Liang, Y. Zhang, T. Jia, C. Cao, L. Kang, W. Xu, and J. Chen, *Appl. Phys. Lett.* **99**, 161113 (2011).
- ²¹C. Kurter, P. Tassin, L. Zhang, T. Koschny, A. P. Zhuravel, A. V. Ustinov, S. M. Anlage, and C. M. Soukoulis, *Phys. Rev. Lett.* **107**, 043901 (2011).
- ²²W. Cao, R. Singh, C. Zhang, J. Han, M. Tonouchi, and W. Zhang, *Appl. Phys. Lett.* **103**, 101106 (2013).
- ²³H. Tao, A. Strikwerda, K. Fan, W. Padilla, X. Zhang, and R. Averitt, *Phys. Rev. Lett.* **103**, 147401 (2009).
- ²⁴W. M. Zhu, A. Q. Liu, X. M. Zhang, D. P. Tsai, T. Bourouina, J. H. Teng, X. H. Zhang, H. C. Guo, H. Tanoto, and T. Mei, *Adv. Mater.* **23**, 1792 (2011).
- ²⁵W. Zhu, A. Liu, T. Bourouina, D. Tsai, J. Teng, X. Zhang, G. Lo, D. Kwong, and N. Zheludev, *Nat. Commun.* **3**, 1274 (2012).
- ²⁶W. Zhang, W. M. Zhu, H. Cai, M.-L. J. Tsai, G.-Q. Lo, D. P. Tsai, H. Tanoto, J.-H. Teng, X.-H. Zhang, and D.-L. Kwong, *IEEE J. Sel. Top. Quantum Electron.* **19**, 4700306 (2013).
- ²⁷Y.-S. Lin, Y. Qian, F. Ma, Z. Liu, P. Kropelnicki, and C. Lee, *Appl. Phys. Lett.* **102**, 111908 (2013).
- ²⁸Z. Han, K. Kohno, H. Fujita, K. Hirakawa, and H. Toshiyoshi, *Opt. Express* **22**, 21326 (2014).
- ²⁹M. Unlu, M. Hashemi, C. Berry, S. Li, S.-H. Yang, and M. Jarrahi, *Sci. Rep.* **4**, 5708 (2014).
- ³⁰P. Pitchappa, C. P. Ho, Y. Qian, L. Dhakar, N. Singh, and C. Lee, *Sci. Rep.* **5**, 11678 (2015).
- ³¹P. Pitchappa, C. P. Ho, L. Cong, R. Singh, N. Singh, and C. Lee, "Reconfigurable Digital Metamaterial for Dynamic Switching of Terahertz Anisotropy," *Adv. Opt. Mater.* (published online, 2015).
- ³²X. J. He, Q. X. Ma, P. Jia, L. Wang, T. Y. Li, F. M. Wu, and J. X. Jiang, *Integr. Ferroelectr.* **161**, 85 (2015).
- ³³P. Pitchappa, M. Manjappa, C. P. Ho, R. Singh, N. Singh, and C. Lee, "Active Control of Electromagnetically Induced Transparency Analog in Terahertz MEMS Metamaterial," *Adv. Opt. Mater.* (published online, 2016).
- ³⁴R. Singh, I. Al-Naib, D. R. Chowdhury, L. Cong, C. Rockstuhl, and W. Zhang, *Appl. Phys. Lett.* **105**, 081108 (2014).
- ³⁵N. Katsarakis, T. Koschny, M. Kafesaki, E. Economou, and C. Soukoulis, *Appl. Phys. Lett.* **84**, 2943 (2004).
- ³⁶R. Singh, C. Rockstuhl, F. Lederer, and W. Zhang, *Phys. Rev. B* **79**, 085111 (2009).
- ³⁷P. Pitchappa, C. P. Ho, L. Dhakar, and C. Lee, *Optica* **2**, 571 (2015).
- ³⁸F. Ma, Y.-S. Lin, X. Zhang, and C. Lee, *Light: Sci. Appl.* **3**, e171 (2014).
- ³⁹Y. Qian, L. Lou, M. J. Tsai, and C. Lee, *Appl. Phys. Lett.* **100**, 113102 (2012).
- ⁴⁰P. Singh, C. G. Li, P. Pitchappa, and C. Lee, *IEEE Electron Device Lett.* **34**, 987 (2013).
- ⁴¹I. Al-Naib, E. Hebestreit, C. Rockstuhl, F. Lederer, D. Christodoulides, T. Ozaki, and R. Morandotti, *Phys. Rev. Lett.* **112**, 183903 (2014).